Acquisition of a hybrid E/M state is essential for tumorigenicity of basal breast cancer cells

Acquisition of a hybrid E/M state is essential for tumorigenicity of basal breast cancer cells

Cornelia Kröger[a], Alexander Afeyan[a,b], Jasmin Mraz[a,c], Elinor Ng Eaton[a], Ferenc Reinhardt[a], Yevgenia L. Khodor[d], Prathapan Thiru[a], Brian Bierie[a], Xin Ye[a,e], Christopher B. Burge[d], and Robert A. Weinberg[a,f,g,1]

[a]Whitehead Institute for Biomedical Research, Cambridge, MA 02142; [b]Department of Molecular and Cellular Biology, Harvard College, Harvard University, Cambridge, MA 02138; [c]Section of Transplantation Immunology, Department of Surgery, Medical University of Vienna, 1090 Vienna, Austria; [d]Biology Department, Massachusetts Institute of Technology, Cambridge, MA 02142; [e]Department of Discovery Oncology, Genentech Inc., South San Francisco, CA 94080; [f]Biology Department, Massachusetts Institute of Technology, Cambridge, MA 02142; and [g]Ludwig Center for Molecular Oncology, Massachusetts Institute of Technology, Cambridge, MA 02139

Contributed by R. A. Weinberg, February 20, 2019 (sent for review August 9, 2018; reviewed by Filippo G. Giancotti and Arthur M. Mercurio)

Carcinoma cells residing in an intermediate phenotypic state along the epithelial–mesenchymal (E–M) spectrum are associated with malignant phenotypes, such as invasiveness, tumor-initiating ability, and metastatic dissemination. Using the recently described CD104^{+}/CD44^{hi} antigen marker combination, we isolated highly tumorigenic breast cancer cells residing stably—both in vitro and in vivo—in an intermediate phenotypic state and coexpressing both epithelial (E) and mesenchymal (M) markers. We demonstrate that tumorigenicity depends on individual cells residing in this E/M hybrid state and cannot be phenocopied by mixing two cell populations that reside stably at the two ends of the spectrum, i.e., in the E and in the M state. Hence, residence in a specific intermediate state along the E–M spectrum rather than phenotypic plasticity appears critical to the expression of tumor-initiating capacity. Acquisition of this E/M hybrid state is facilitated by the differential expression of EMT-inducing transcription factors (EMT-TFs) and is accompanied by the expression of adult stem cell programs, notably, active canonical Wnt signaling. Furthermore, transition from the highly tumorigenic E/M state to a fully mesenchymal phenotype, achieved by constitutive ectopic expression of Zeb1, is sufficient to drive cells out of the E/M hybrid state into a highly mesenchymal state, which is accompanied by a substantial loss of tumorigenicity and a switch from canonical to noncanonical Wnt signaling. Identifying the gatekeepers of the various phenotypic states arrayed along the E–M spectrum is likely to prove useful in developing therapeutic approaches that operate by shifting cancer cells between distinct states along this spectrum.

cancer stem cells | EMT | E/M hybrid state | EMT-TFs | Wnt signaling

Intratumor phenotypic heterogeneity poses a major challenge for designing effective therapies for high-grade carcinomas including breast cancers (1). In the case of carcinomas, much of this heterogeneity within the neoplastic cell populations is due to the operations of the cell-biological program termed the epithelial–mesenchymal transition (EMT). By enabling phenotypic cell plasticity, an EMT program can shift carcinoma cells to various phenotypic states arrayed along the epithelial (E) to mesenchymal (M) spectrum (2, 3). In the context of carcinoma development, epithelial carcinoma cells that have activated their EMT programs gain, in addition to certain mesenchymal traits, stem-like characteristics, increased drug resistance, invasiveness, and metastatic ability (4). Recent reports have concluded that in order for tumor progression and metastasis to proceed, the activation of an EMT program needs to be transient and reversible (5–7).

A cohort of contextual signals governs activation of EMT programs and their associated phenotypes within carcinoma cells. Signals such as TGF-β and Wnt ligands that these cells receive from their microenvironment work together with cell-intrinsic signaling to provoke the expression of various EMT-inducing transcription factors (EMT-TFs), such as Zeb1, Twist, and Snail (8–10). Wnt ligands, in particular, can activate β-catenin–dependent canonical as well as β-catenin–independent noncanonical Wnt signaling. Canonical Wnt signaling is preferentially activated in stem cells (11), whereas noncanonical Wnt signaling, which can be further subdivided into calcium-dependent and planar cell polarity (PCP) downstream signaling pathways, has been associated with migration and invasion (12, 13). The specific downstream signaling responses are highly dependent on the cellular context and on the identities of individual Wnt ligands, receptors, and coreceptors and have been reported to exert both oncogenic and tumor suppressive effects (14–17).

Previous reports have indicated that stable residence in a completely E or a completely M state is incompatible with the acquisition of stemness (6, 18). Instead, as recent data show, tumor cells with the highest stem cell capabilities reside in a hybrid E/M state (19). Such observations are compatible with two alternative mechanistic hypotheses: cells must exhibit phenotypic plasticity to move between these various states to acquire stemness, or alternatively, residence in the intermediate E/M state is critical to stemness, independent of phenotypic plasticity. Finally, computational models and in vitro data argue that under certain in vitro conditions, carcinoma cells can reside stably in such an E/M state (2, 20–23).

To address these questions, we used the marker combination CD104/CD44 to isolate E, hybrid E/M, and M cell populations (19) and tracked their E and M status during propagation in vitro

Significance

As carcinoma cells progress toward high-grade malignancy, they often if not invariably activate the cell-biological program termed the epithelial–mesenchymal transition (EMT). We discovered that, both in vitro and in vivo, certain breast cancer cells can reside stably and thus with low cell plasticity in a highly tumorigenic, hybrid epithelial/mesenchymal state driven by Snail and canonical Wnt signaling. However, if such cells are forced into a fully mesenchymal state, this results in a poorly tumorigenic cell population under the control of Zeb1 and noncanonical Wnt signaling. These findings suggest that the design of future therapeutic approaches will need to consider the various subpopulations of carcinoma cells that reside at various positions along the E–M spectrum.

Author contributions: C.K. and R.A.W. designed research; C.K., A.A., J.M., E.N.E., and F.R. performed research; C.K., B.B., and X.Y. contributed new reagents/analytic tools; C.K., Y.L.K., P.T., and C.B.B. analyzed data; and C.K. and R.A.W. wrote the paper.

Reviewers: F.G.G., MD Anderson Cancer Center; and A.M.M., University of Massachusetts.

The authors declare no conflict of interest.

Data deposition: The data reported in this paper have been deposited in the Gene Expression Omnibus (GEO) database, https://www.ncbi.nlm.nih.gov/geo (accession no. GSE119149).

[1]To whom correspondence should be addressed. Email: weinberg@wi.mit.edu.

This article contains supporting information online at www.pnas.org/lookup/suppl/doi:10.1073/pnas.1812876116/-/DCSupplemental.

Published online March 25, 2019.

and following xenograft implantation in mice. Furthermore, to identify the critical stemness pathways that drive entrance into the various cell states along the E–M spectrum, we analyzed the cells for cancer stem cell (CSC) markers and active CSC signaling programs.

We discovered that both in vitro and in vivo, certain breast cancer cells can reside stably and with low cell plasticity in a highly tumorigenic hybrid E/M state, which is driven by the Snail EMT-TF and canonical Wnt signaling. Forcing such cells into an entirely mesenchymal state, achieved by driving them through a complete EMT program, results in a poorly tumorigenic cell population under the control of Zeb1 and noncanonical Wnt signaling.

Results

Maintenance of the Hybrid E/M State in Vitro and in Vivo. The importance of cell plasticity in driving the transition of poorly tumorigenic epithelial carcinoma cells into highly aggressive CSCs via induction of an EMT has been well described (1, 2, 24). Relatively little is known about the specific cell states along the E-to-M spectrum in which CSC populations reside and the role that cell plasticity plays in enabling them to function effectively as tumor-initiating cells. To address these questions, we employed the well-characterized human mammary epithelial (HMLER) cell culture model. These cells were immortalized by forced expression of hTERT and were then transformed by introduction of SV40 early-region genes and the *HRAS* V12 oncogene (25, 26).

To enrich for tumor cell populations with differing E versus M traits, we FACS-sorted HMLER cells through multiple successive cycles using the recently described CD104/CD44 cell surface marker combination (19) (*SI Appendix*). This resulted in the highly pure E ($CD104^{+}CD44^{low}$), hybrid E/M ($CD104^{+}CD44^{hi}$), and xM ($CD104^{-}CD44^{hi}$) tumor cell subpopulations (Fig. 1*A*); the latter notation (xM) refers to cells that entered into a highly mesenchymal state with no apparent retention of epithelial markers, a state that we also refer to as the "extreme mesenchymal state."

We set out to characterize these populations in vitro for EMT-associated marker expression by FACS, immunofluorescence (IF), Western blot, and qPCR analyses (Fig. 1 *A–D*). As anticipated, E/M cells exhibited a mixture of E and M traits, including the simultaneous expression of CD104 and CD44 together with other E and M markers. Analysis of the mRNA transcript and protein levels for keratins (Krts), 5 and 8, and pan-cytokeratin IF staining revealed down-regulation of Krts in E/M cells relative to the E cells. In addition, the E/M cells lost all expression of E-cadherin mRNA and protein and gained instead expression of the mesenchymal marker vimentin and the Zeb1 EMT-TF (Fig. 1 *A–D*).

As gauged by Western blotting, total cellular Zeb1 protein levels were not significantly different between E/M and xM cells. IF as well as Western blot analysis of cell fractions revealed, however, that Zeb1 was predominantly localized in the nuclei of xM cells relative to the E/M cells, where it was also found in the cytoplasm. QPCR data demonstrated increased *ZEB1* transcript levels in cells that had undergone a complete EMT and entered into the highly mesenchymal xM state (Fig. 1*D*). These results were confirmed by comparing the HMLER cell system to transcript data of SUM159 human breast cancer cells that were sorted for CD104+ and CD104− cell populations, these being E/M and xM, respectively. SUM159 cells in the xM state expressed twice as much *ZEB1* as E/M cells (*SI Appendix*, Fig. S6*B*) (19). Hence, the transcriptional functions of Zeb1 function, which is often depicted as the master regulator of the EMT program, appeared to be correlated largely with entrance into the xM cell state.

Western blot analyses of protein levels of the Slug and Twist EMT-TFs did not reveal major differences between the E, E/M, and xM populations, whereas Twist levels were elevated in both E/M and xM cells relative to E cells (Fig. 1*C*). Interestingly, levels of the Snail protein, which is known to be regulated posttranslationally (27), were significantly elevated (fivefold) in E/M cells relative to the xM cells (Fig. 1*C*), in contrast to corresponding transcript levels, which only increased 1.5-fold relative to E or xM cells (Fig. 1*D*). A similar elevation of around twofold in *Snail* transcript levels could be observed in SUM159 E/M cells compared with xM cells (*SI Appendix*, Fig. S6*B*) (19). These observations revealed a differential expression of the EMT-TFs as cells move along the E–M spectrum, with Snail being up-regulated in the hybrid E/M cells and down-regulated in the xM cells, whereas high nuclear Zeb1 expression was observed in the xM cells, as demonstrated by IF (Fig. 1*B*; see Fig. 4*D*). These findings are summarized in Fig. 1*E*.

Because constitutive overexpression of Snail in various breast cancer cell lines has been associated with low tumorigenicity (6, 18), we analyzed the tumorigenicity and properties of tumors initiated by the E, E/M, and xM cells (Fig. 1*F*). Injections of cells into the mammary fat pad revealed that the highly purified E cells and the xM cells did not form robustly growing tumors in contrast to cells exhibiting the hybrid E/M phenotype. In particular, the E/M tumors were ∼10-fold larger than the tumors formed by the implanted E and xM cells (Fig. 1*F*). s.c. implantation of these cell populations at limiting dilutions, performed to determine the frequency of tumor-initiating CSCs, indicated that the frequency of CSCs in the E/M population was 122- and 3.7-fold higher than the corresponding CSC frequencies in E and xM populations, respectively (*SI Appendix*, Fig. S1*C*). This reinforced the conclusion, previously made by others (5–7, 28), that the residence of carcinoma cells in phenotypic states at the two ends of the E–M spectrum renders them less capable of functioning as tumor-initiating CSCs. Taken together, the experiments also suggested that high Snail expression per se was not linked to low tumorigenicity.

The observed differences in tumor-initiating ability were accompanied by dramatic differences in tumor histology. H&E staining revealed that the tumors formed by both the implanted E and E/M tumors resembled carcinomas: E tumors presented an adenocarcinoma-like morphology, whereas E/M tumors exhibited morphological features of poorly differentiated carcinomas. The small xM tumors exhibited a highly sarcomatoid morphology, with less closely packed tumor cells and high infiltration by stromal cells (Fig. 1*G*). Moreover, the tumors formed by xM carcinoma cells displayed a dramatic infiltration of myofibroblasts, marked by α-smooth muscle actin (α-SMA) staining of mouse stromal cells, whereas the carcinoma cells (visualized by SV40 LT staining) in these tumors exhibited elevated nuclear Zeb1 staining compared with cells in the E/M tumors (Fig. 1*G* and *SI Appendix*, Fig. S1*E*). We confirmed that expression of E-cadherin and Krt5 was absent and vimentin expression elevated in tumors formed by the implanted E/M and xM cells (Fig. 1*G*).

These data further corroborate our previously described IF analyses of these various cells in vitro. In particular, the increased Zeb1 expression observed in vitro and in vivo in xM cell-derived tumors suggested that Zeb1 expression was the key regulator of the transition to the highly mesenchymal cell state. We noted that myofibroblast-rich stromal microenvironments, such as that recruited by the xM carcinoma cells, have been shown to secrete high levels of the EMT-inducing factor TGF-β1 (29, 30). This suggests that xM tumor cells recruit a stromal microenvironment favorable to maintaining their own highly mesenchymal state.

We asked if residence in the E/M cell state was sufficient for tumorigenicity and speculated that pure E/M populations residing stably in this mixed phenotypic state possess tumor-initiating potential, doing so independent of their exhibiting phenotypic plasticity along the E–M axis. To address this, we analyzed the extent of plasticity of the E/M tumor cells, more specifically, their ability to remain in the E/M state and retain expression of the CD104 epithelial marker while growing within tumors in vivo.

Analysis of 10 individual tumors arising from implanted E/M cells indicated that seven of these robustly growing tumors contained E/M carcinoma cells that did not alter their high levels

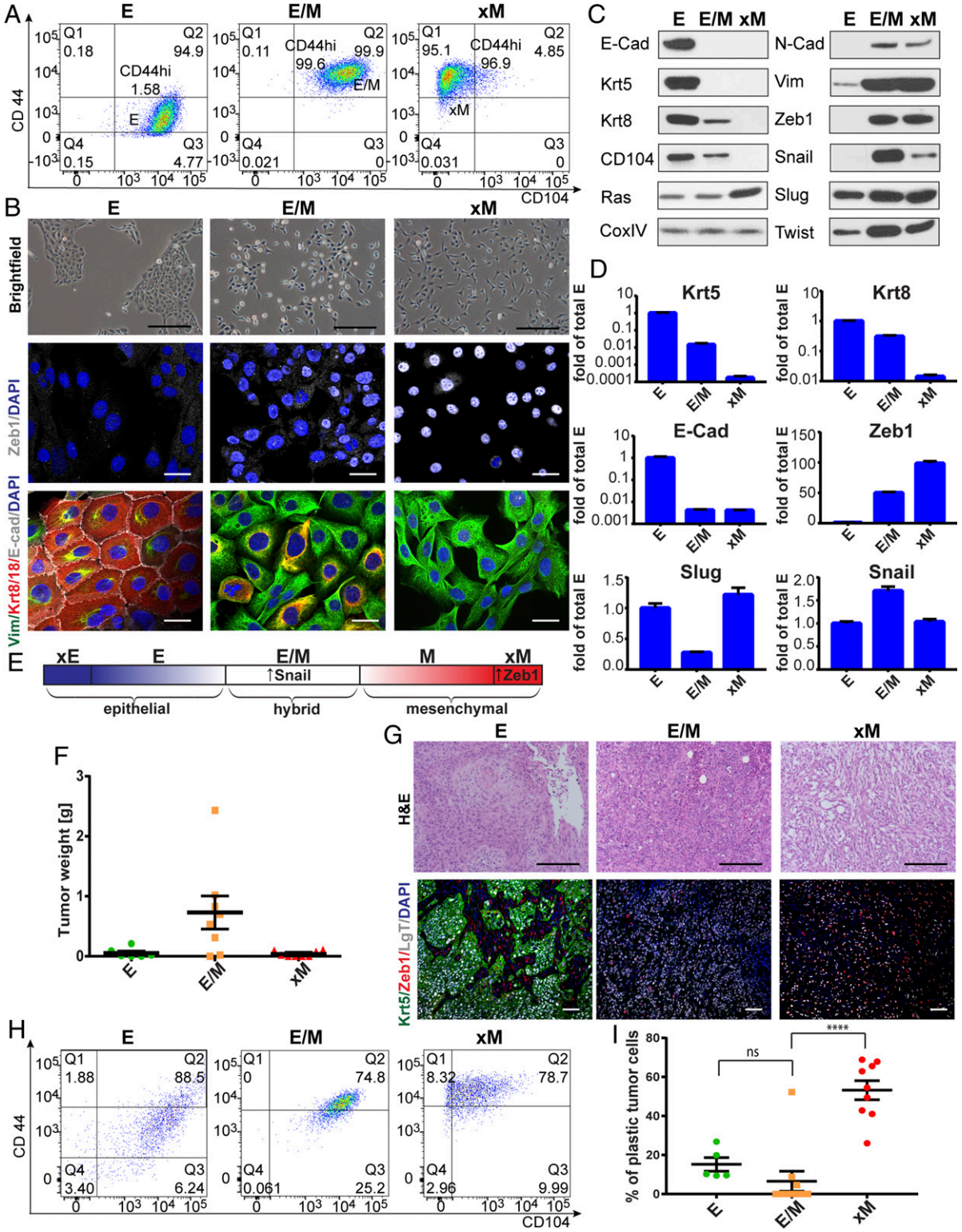

Fig. 1. The stable hybrid E/M state is enriched for CSCs and is maintained in vivo. (*A*) FACS profiles for CD104 and CD44 of HMLER E, E/M, and xM populations. (*B*) Representative images of E, E/M, and xM cells by phase contrast (brightfield) and IF staining for Zeb1 and E-Cad/Vim/Krt8/18. Nuclei are visualized by DAPI. (*C*) Representative Western blot analysis of E, E/M, and xM cells for epithelial and mesenchymal markers of three independent lysates. (*D*) Quantitative PCR assessing levels of mRNA encoding various markers of the E, E/M, and M phenotypic states. (*E*) Model of the different E–M cell states based on the findings in *Results*. Snail and Zeb1 indicate the EMT-TFs that are expressed at highest levels (in the E/M state in the case of Snail) or nuclear localization (in the xM state in the case of Zeb1). (*F*) Assessment by tumor weight of tumorigenicity and tumor growth ability of 1×10^5 E, E/M, and xM cells injected orthotopically. Xenografts were extracted and analyzed 8 wk postimplantation. (*G*) Analysis of E, E/M, and xM tumor sections using H&E and IF staining for Krt/Zeb1. SV40 LgT staining was used to differentiate tumor cells from mouse stromal cells. Nuclei are visualized by DAPI staining. (*H*) FACS analysis for CD104 and CD44 expression of dissociated neoplastic cells of E, E/M, and xM tumors. (*I*) Quantitative analysis of tumor cells that have altered their original in vitro CD104/CD44 marker profile while growing in vivo over a period of 8 wk. ****$P < 0.00005$ (two-tailed *t* test). Data are presented as mean ± SEM. Scale bars, brightfield; H&E, 10 μm; IF, 1 μm in *B* and 2 μm in *G*.

of $CD104^{+}/CD44^{hi}$ expression, as determined by FACS, and therefore remained entirely in an E/M state; the remaining tumors arising from implanted E/M cells contained carcinoma cells that had shifted spontaneously to a full $CD104^{-}/CD44^{hi}$ mesenchymal phenotype (Fig. 1 *H* and *I*). The relatively low degree of plasticity of the cells in the tumors retaining an E/M phenotype was further supported by the observation that the level of CD104 expression was uniform among all of the E/M cells within these E/M-initiated tumors, as indicated by the narrowness of the CD104 peak in the FACS plots (*SI Appendix*, Fig. S1*G*). These data are consistent with the notion that residence in the E/M state was, on its own, sufficient for these cells to exhibit tumor-forming abilities.

The observations cited above provided the first indication that cell plasticity along the E–M axis could be uncoupled from the ability of tumor cells to initiate robustly growing tumors. Stated differently, the E/M cell population, which contained almost all of the tumor-initiating CSCs, did not seem to rely on E–M plasticity for tumorigenicity, at least as determined by CD104/CD44 marker analysis (Fig. 1 *F*–*I*).

Effects of Blocking Plasticity on Tumor Initiation and Outgrowth. The apparent requirement for tumorigenicity of the concomitant expression by a cell population of E and M traits—as displayed by the E/M cells—was compatible with two alternative mechanistic hypotheses: (*i*) the E and M traits could be expressed by distinct subpopulations of carcinoma cells, each expressing one or the other phenotype and coexisting within the same tumor, or (*ii*) coexpression of E and M phenotypes within individual cells, as exemplified by the E/M cells described above, sufficed for tumorigenicity. To resolve between these alternatives, we asked whether the highly tumorigenic E/M cells coexpressing E and M markers could be replaced by a mixture of nonplastic xE and xM cells. Hypothetically, these two cell populations, working together, should contribute the E and M traits that might be required, in aggregate, to form robustly growing tumors, demonstrating an interdependence of the E and M subpopulations for successful tumor formation.

Specific strategies for creating such nonplastic cells were suggested by previous studies (5–7, 28). Thus, knocking down the *ZEB1* transcript with shRNA constructs resulted in cells that did not transit out of the highly epithelial state (28, 31). Other work demonstrated that forced constitutive overexpression of *ZEB1* would result in poorly tumorigenic, highly mesenchymal cells exhibiting low plasticity.

To trap cells in an entirely epithelial state, we used the CRISPR/Cas9 technology to completely eliminate Zeb1 expression in a population of single-cell–derived clones (SCC) of E cells. These E-SCC-Zeb1KO cells did not express Zeb1 and were termed xE-SCC-Zeb1KO cells (*SI Appendix*).

Alternatively, to generate cells that were held in the xM state, we used an introduced expression vector that drives constitutive overexpression of Zeb1 in cells that were subsequently isolated as a single-cell clone, terming these the xM-SCC-Zeb1. These cells exhibited 20-fold higher Zeb1 expression relative to the corresponding M parental cells (Fig. 2*A* and *SI Appendix*, Fig. S2*F*).

We considered the E-SCC-Zeb1KO cells and the xM-SCC-Zeb1–overexpresser cells as being trapped in their respective phenotypic states at the two ends of the E–M spectrum; we confirmed this by FACS analysis using CD104 and CD44 marker expression (Fig. 2*B*). Comparing the xE and xM to the more heterogeneous E and M parental populations, we confirmed our hypothesis that a reduction of plasticity in either the xE or xM populations, each residing at an end of the E–M spectrum, resulted in reduced tumorigenicity. We observed a drop in tumor incidence from 66 to 13.5% when comparing E to xE tumor-bearing hosts, respectively. Similarly, 100% of the mice implanted with the M cells developed tumors compared with 13.5% of the mice bearing tumors seeded by the xM-SCC-Zeb1 cells; in addition, the CSC frequency in xM-SCC-Zeb1 cells dropped 63-fold relative to the parental M cells (Fig. 2*C* and *SI Appendix*, Figs. S1*A* and S4*C*). The differences in tumor size were even more dramatic: tumors generated by xM-SCC-Zeb1 populations were 30-fold smaller than the M parental controls; similarly, the tumors generated by xE-SCC-Zeb1KOcells were 20-fold smaller than corresponding E cells. We also confirmed, using FACS analysis of dissociated tumor cells, that we could indeed prevent the majority of cells lodged in the extreme ends of the E–M spectrum from exiting their respective xE or xM states while growing in vivo (Fig. 2*E*). Taken together, these observations provided further substantiation that residence in these xE and xM states is counterproductive for tumor formation.

Histopathological analysis with H&E staining and IF of Krt5 and Zeb1 confirmed the phenotype of the various cell populations (Fig. 2*D*). Both E and xE cells immunostained positive for Krt5. The xE-SCC-Zeb1KO/xE tumors uniformly lacked detectable Zeb1 expression, whereas E control tumors demonstrated partial up-regulation of Zeb1 in individual cells (*SI Appendix*, Fig. S2*H*). Tumors arising from the xM-SCC mesenchymal control cells were Krt5-negative and stained positive for Zeb1. Moreover, this strong Zeb1 IF staining confirmed the Zeb1 overexpression in the few smaller tumors that succeeded in growing out from the implanted xM-SCC-Zeb1 cells (Fig. 2*E* and *SI Appendix*, Fig. S2*H*).

Of central importance, mixing equal proportions of the two extreme xE-SCC-Zeb1KO and xM-SCC-Zeb1 cells before implantation did not result in increased tumor seeding and outgrowth compared with that displayed by the individual xE or xM populations implanted separately (Fig. 2*C*). This demonstrated directly that simple interdependence of distinct E and M cell subpopulations within a tumor, each contributing either E or M functions, could not explain the observed requirement for phenotypically hybrid E/M cells in tumor formation. Stated differently, the coexpression of E and M traits within individual cells appeared to be essential for expression of high tumorigenicity.

Zeb1 Is Required for a Full EMT but Not for Tumor Formation. The above observations extended and supported previous reports indicating that shifts between E and M states are governed by the actions of EMT-TFs (8, 32). Nevertheless, the specific roles of various EMT-TFs in controlling the residence in specific intermediate states along the E–M spectrum are still not well understood. For this reason, we explored the roles of several EMT-TFs in conveying cells into the E–M states described above.

As described above, immunoblot analyses indicated that protein levels of the Snail EMT-TF were significantly up-regulated in the E/M state but not in the xM state. This contrasted with the behavior of Zeb1 expression in the nucleus, which was seen largely in the xM state (Fig. 1 *C*–*E* and *G*; Fig. 4*D*). Accordingly, we hypothesized that Snail was more important for orchestrating the E/M state, whereas Zeb1 was more important for the xM state. To further test this notion, we forced E-SCC-Zeb1KO cells, which on their own resided in the fully epithelial xE state, to activate components of their silent EMT program. Knowing that Snail (Sn) is up-regulated in the E/M state, we introduced a constitutive Snail IRES tdTomato expression vector into both the E-SCC-Zeb1KO cells and the E-SCC controls, generating E-SCC-Zeb1KOSn cells and the E-SCCSn cells.

We confirmed that as anticipated, Zeb1 was not expressed following forced Snail EMT-TF expression in E-SCC-Zeb1KOSn single-cell clones in contrast to its expression in the isogenic E-SCCSn parental control cells (33), whereas nuclear Zeb1 was indeed readily detected in the control isogenic E-SCCSn clones, as determined by nuclear Zeb1 IF staining as well as immunoblotting (*SI Appendix*, Figs. S3*A* and S5 *B* and *C*). Moreover, and most importantly, forced expression of Snail in the ZEB1KO cells pushed these cells from an E state into the hybrid E/M state but failed to move them further into the xM state. This contrasted with the responses of forced Snail expression in the E-SCCSn control cells, which could indeed activate endogenous Zeb1 expression in

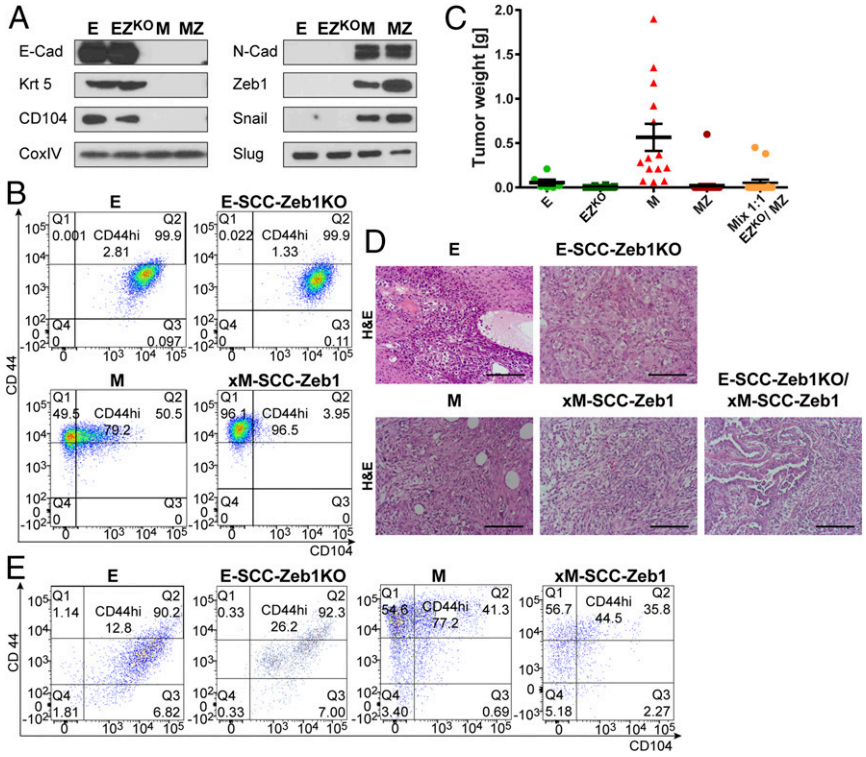

Fig. 2. Blocking plasticity reduces tumor formation and growth in xE and xM cells; this inability cannot be compensated by mixing xE and xM cells before implantation into an orthotopic site. (*A*) Representative Western blot analysis of parental HMLER and trapped xE/xM populations, E, E-SCC-Zeb1KO (EZ^{KO}), M, and xM-SCCZeb1 (MZ) for epithelial and mesenchymal markers (SCC, single-cell clone). (*B*) FACS profiles for CD104 and CD44 of E, E-SCC-Zeb1KO, M, and xM-SCCZeb1 populations before implantation into host mice. (*C*) Assessment of tumorigenicity and tumor growth by tumor weight of orthotopic injection of E, EZ^{KO}, M, MZ, and 1:1 mix of the trapped xE and xM populations. Data are presented as mean ± SEM. (*D*) Analysis of E, E-SCC-Zeb1KO, M, and xM-SCCZeb1 and 1:1 mix of the trapped xE and xM tumor sections using H&E. (*E*) FACS profiles for CD104 and CD44 of E, E-SCC-Zeb1KO, M, and xM-SCCZeb1 expression of dissociated neoplastic cells after they had grown in vivo for 8 wk. (Scale bars, 10 μm.)

response to the actions of the introduced Snail and began to undergo a full EMT (*SI Appendix*, Fig. S3*B*).

This limited movement of the E-SCC-Zeb1KOSn cells from a fully epithelial to the mixed E/M state was most unexpected, since high, experimentally induced levels of Snail expression usually succeeded in our hands in driving cells to the xM fully mesenchymal endpoint (*SI Appendix*, Fig. S3 *A* and *B*). Indeed, after 3 wk of forced Snail expression, the E-SCCSn control cells had undergone a full EMT, which was indicated by their mesenchymal spindle-like cell morphology in monolayer culture, acquisition of a $CD104^{-}CD44^{hi}$ antigen phenotype, and EMT marker analysis by Western blot (Fig. 3 *A* and *B* and *SI Appendix*, Fig. S5 *B* and *C*). In stark contrast, the E-SCC-Zeb1KOSn cells continued to express their hybrid E/M $CD104^{+}CD44^{hi}$ phenotype (Fig. 3*B*).

We concluded that Snail could function in the absence of Zeb1 to push cells from an xE state into the E/M, hybrid phenotypic state; however, Zeb1 function appeared to be necessary to enable the further Snail-induced transition to a xM phenotype. The continued long-term residence of the E-SCC-Zeb1KOSn cells in the E/M state revealed that they could indeed reside indefinitely in this hybrid phenotypic state. Alternative EMT inducers, such as other EMT-TFs (Twist and Slug) or exposure to TGF-β1, a potent EMT inducer (8), elicited the same limited response in the E-SCC-Zeb1KO cells (*SI Appendix*, Fig. S5).

Furthermore, we could confirm that this was not an idiosyncrasy of the HMLER cell system. Sum149 cells, modified in the same way as the E-SCC-ZEB1KO cells, displayed the same behavior. Sum149-SCC treated with TGF-β1 progressed to an xM state, whereas Sum149-SCC-ZEB1KO cells treated with TGF-β1 could only progress into an E/M state. This provided further support to the notion that Zeb1 expression is needed for completion of an EMT program and thus generation of highly mesenchymal xM cells (*SI Appendix*, Fig. S4*A*).

We proceeded to test the tumor-forming abilities of the cells described above (Fig. 3 *C* and *D*). The epithelial clones (E-SCC and E-SCC-Zeb1KO) and the constitutive Snail-expressing mesenchymal cells (E-SCCSn) displayed poor tumor-initiating and outgrowth ability, revealing again that residence in either the xE or xM states was incompatible with efficient tumor initiation. In contrast, the E-SCC-Zeb1KOSn cells, which resided stably in an E/M state, produced tumors that grew up to a 200-fold larger size and displayed a 37-fold higher tumor-initiating frequency relative to the E-SCC and E-SCC-Zeb1KO controls, as gauged by limiting-dilution experiments (Fig. 3*D*). Most strikingly, the E-SCC-Zeb1KOSn cells retained their E/M phenotype in vivo, as determined by their $CD104^{+}CD44^{hi}$ FACS phenotype (*SI Appendix*, Fig. S4*C*). Furthermore, IF of tumor sections clearly demonstrated that these cells continued to express high levels of the epithelial markers E-Cad and Krt5, despite high Snail expression (Fig. 3*E*). Consequently, this Zeb1 KO, Snail-overexpressing cell population displayed low plasticity along the E–M axis relative to the respective E (E-SCC and E-SCC-Zeb1KO) and xM like controls (E-SCCSn) but were nonetheless highly tumorigenic (Fig. 3 *B*–*D* and *SI Appendix*, Fig. S4*C*). These observations, on their own, indicated that stable residence in the hybrid E/M state without detectable plasticity was compatible with high tumorigenicity, i.e., the ability to seed new tumors and to drive the rapid growth of those tumors. Stated differently, residence in the E/M state, rather than phenotypic

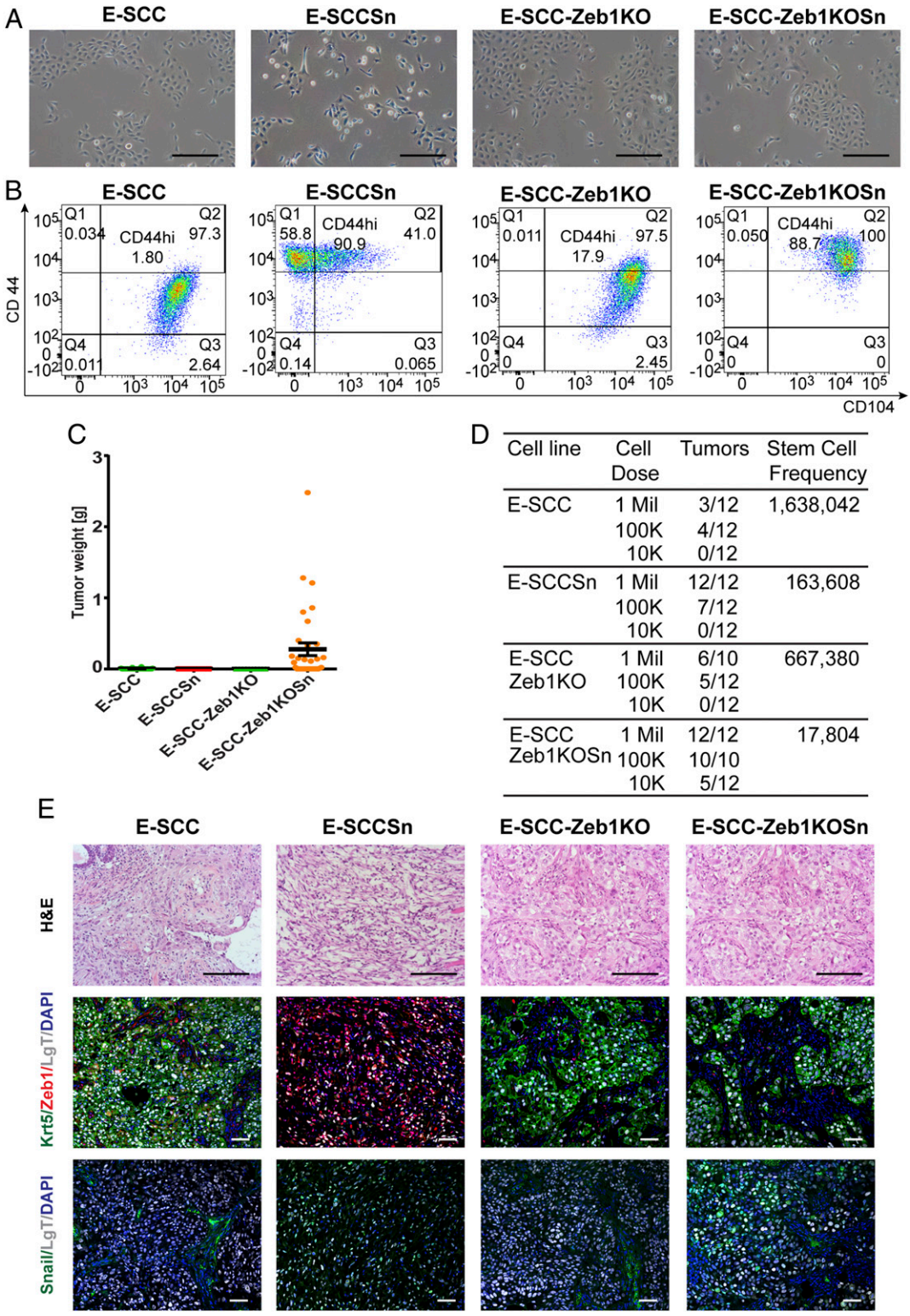

Cell line	Cell Dose	Tumors	Stem Cell Frequency
E-SCC	1 Mil	3/12	1,638,042
	100K	4/12	
	10K	0/12	
E-SCCSn	1 Mil	12/12	163,608
	100K	7/12	
	10K	0/12	
E-SCC Zeb1KO	1 Mil	6/10	667,380
	100K	5/12	
	10K	0/12	
E-SCC Zeb1KOSn	1 Mil	12/12	17,804
	100K	10/10	
	10K	5/12	

Fig. 3. Zeb1 is needed for a complete EMT, but the hybrid E/M cell state is sufficient for tumor formation. (*A*) Representative images of cell morphology of E-SCC, E-SCCSn, E-SCC-Zeb1KO, and E-SCC-Zeb1KOSn cells by phase contrast (brightfield) microscopy. (*B*) FACS profiles for CD104 and CD44 of E-SCC, E-SCCSn, E-SCC-Zeb1KO, and E-SCC-Zeb1KOSn populations. (*C*) Assessment of tumorigenicity and tumor growth by tumor weight of orthotopic injection E-SCC, E-SCCSn, E-SCC-Zeb1KO, and E-SCC-Zeb1KOSn populations. Data are presented as mean ± SEM. (*D*) Differences in tumor-initiating ability of E-SCC, E-SCCSn, E-SCC-Zeb1KO, and E-SCC-Zeb1KOSn cells upon transplantation at limiting dilutions into NOD/SCID mice. (*E*) Analysis of E-SCC, E-SCCSn, E-SCC-Zeb1KO, and E-SCC-Zeb1KOSn tumor sections using H&E and IF staining for Krt/Zeb1 or Snail. LgT staining was used to differentiate tumor cells from mouse stromal cells. Nucleus is visualized by DAPI staining. (Scale bars, brightfield; H&E, 10 μm; IF, 2 μm in *E*.)

plasticity (involving movement between phenotypic states along the E–M spectrum), was critical to tumor-initiating ability.

To further confirm that Zeb1 expression was critical for cells to advance from the E/M state to the fully mesenchymal xM state we introduced a CRISPR KO-resistant mutant form of the *ZEB1* gene (*ZEB1*mt) into both the E-SCC-Zeb1KO and E-SCC-Zeb1KOSn cells. As observed by FACS, we could reverse the effects of the ZEB1 KO and residence in the E/M state. Both E-SCC-Zeb1KO and E-SCC-Zeb1KOSn cells with restored Zeb1 expression were indeed now able to progress into a highly mesenchymal xM state (*SI Appendix*, Fig. S5*A*). Hence, expression of Zeb1 was sufficient to drive cells into the xM phenotypic state and to maintain residence in this state.

Because the EMT-TF Snail was highly expressed in the spontaneously formed E/M subpopulation of HMLER cells, we undertook to determine whether the plasticity between cell states and the E/M state was dependent on ongoing Snail expression. For this purpose, we generated with CRISPR/Cas9 Snail KO HMLER cells (E-SCC-SnKO and xM-SCC-SnKO). The E-SCC-SnKO cells were able to undergo all stages of an EMT upon TGF-β1 treatment or Zeb1 overexpression (*SI Appendix*, Fig. S5). However, similar to their E-SCC-Zeb1KO counterparts, without these external stimuli, these cells remained in an xE state with low tumor-forming capability. The same was true for the M-SCC-SnKO cells (*SI Appendix*, Fig. S4*B*). This indicated that Snail KO enabled cells to remain in their existing xE or xM states and hindered them from moving spontaneously into the far more tumorigenic E/M state.

To summarize, these various observations point to the essential role of Zeb1 in permitting the progression of the studied cells to an xM state. Furthermore, the xM state itself was not necessary for tumor formation or growth, because E/M cells were sufficient to initiate tumor formation. Snail, an important driver of EMT and stemness in certain breast cancers (34), was highly up-regulated in the E/M state and, when knocked out in both the E-SCC or M-SCCs, resulted in maintenance of their residence in the xE or xM state with preservation of low tumorigenicity.

Transition from an E/M to an xM State Results in a Switch from Canonical Wnt to Noncanonical Wnt Signaling Maintained by Wnt5a. To discover signaling pathways that define phenotypically distinct states along the E-to-M spectrum and are necessary for maintaining residence in these states, we clustered transcriptome analyses of the different E, E/M, and xM cell states. In doing so, we identified several gene clusters that were differentially expressed between the E, E/M, and xM populations in HMLER cells (*SI Appendix*, Fig. S6*A*). Most prominent among these was the differential expression of EMT-TFs as described above and components of the Wnt pathway in HMLER and Sum159 cells (*SI Appendix*, Fig. S6*B*). The canonical Wnt ligands WNT7A and WNT7B were elevated in both cell populations that expressed epithelial markers, i.e., the E and E/M cells. In stark contrast, in the xM cells, the transcript levels of WNT7A and WNT7B were down-regulated 20- and 7.5-fold, respectively, whereas the noncanonical Wnt ligand WNT5A was up-regulated almost 90-fold. This drastic up-regulation aligns with transcriptome data from SUM159 cells sorted for CD104+ E/M and CD104− xM populations, which demonstrated a 500-fold relative increase in WNT5A transcript in the CD104− xM cells (19).

Further analysis of the transcriptomes of these various cells also revealed that coreceptors of canonical (LRP5) and noncanonical (ROR2) Wnt signaling were elevated in E/M and xM cells, respectively (*SI Appendix*, Fig. S6*B*). In light of the fact that cognate Wnt receptors were expressed in these two cell states, we concluded that the cited Wnts operated in both cases to drive autocrine signaling. Thus, the E and E/M states appear to be associated with canonical Wnt signaling, whereas the xM cells appeared to be associated with noncanonical Wnt signaling. We confirmed that transcript levels reflected the levels of encoded proteins by Western blot analyses (Fig. 4*A*).

To determine if the canonical Wnt7a/Wnt7b ligands were indeed functionally important for HMLER tumor formation, we tested whether blocking their downstream signaling affected tumor growth. Both Wnt7a and Wnt7b have been shown to signal through the canonical Wnt receptor Frizzled-8 (Fz8) (35). To test the importance of these two ligands for tumorigenicity, we used the doxycycline-(Dox)-inducible decoy receptor Fz8 cysteine-rich domain (CRD) (36). We injected Fz8-CRD-expressing epithelial HMLERs into mammary fat pads. After 4 wk, 50% of the mice were treated with Dox to block canonical Wnt signaling; 4 wk later, we observed an eightfold reduction in tumor size in mice treated with Dox compared with untreated mice (Fig. 4*B*). Histopathological analysis of Dox-treated tumors showed an increased infiltration of inflammatory cells and dying tumor cells compared with untreated tumors (Fig. 4*C*). By quenching all Wnt ligand–receptor interactions with the Fz8-CRD decoy construct, we confirmed the significance of ongoing Wnt signaling for robust tumor growth in the HMLER cell system.

Canonical Wnt signaling has been associated with stemness and breast cancer and can be gauged by the translocation of β-catenin to the nucleus, where it activates various downstream targets (16, 17, 37). Upon cell fractionation we could detect nuclear β-catenin by Western blots in all HMLER cells (Fig. 4*D*). GSK-3β inhibits β-catenin function in canonical Wnt signaling on two levels. In the nucleus it blocks β-catenin function by forming an inactive complex (38), whereas in the cytoplasm it phosphorylates β-catenin at its serine 33 and 37 and threonine 41 residues to mark it for degradation by the ubiquitin–proteasome complex (39). Consistent with these observations, we could detect by immunoblot twofold increased nuclear GSK-3β in xM cells compared with E and E/M cells (Fig. 4*D*), in addition to an up-regulation of phosphorylated β-catenin (P-β-catenin) using a serine 33 and 37 and threonine 41 phospho-specific antibody (Fig. 4*E*). Downstream signaling of canonical Wnt was monitored by LRP6 phosphorylation, MET, and TCF1 levels. TCF1 (40) was found to be strongly (~fivefold) up-regulated in the E/M cells relative to xE and xM cells (Fig. 4*E*). This indicated that the stemness-promoting canonical Wnt signaling is up-regulated in the tumorigenic E/M cells and down-regulated in xM cells.

We previously reported that Wnt5a—an activator of noncanonical signaling (15)—was expressed in HMLER-derived mesenchymal cells and that downstream targets of the noncanonical signaling pathway were activated (41). Consistent with this, xM cells, as defined by their $CD104^{-}/CD44^{+}$ FACS profile, expressed high Wnt5a levels as detected by Western blot relative to the E/M cells (Fig. 4*A*), suggesting that HMLER cells switched from canonical to noncanonical autocrine Wnt signaling upon transitioning from an E/M to the xM state.

In more detail, Wnt5a signaling can activate two major noncanonical downstream effector pathways: the PCP and the Ca^{2+} signaling pathways (15). Therefore, we tested if either pathway was activated in E, E/M, and xM cells. We could report that Ca^{2+}-dependent downstream signaling was active in both E/M and xM cells, in contrast to E cells, as revealed by Western blot analysis using phospho-specific antibodies for functionally active PLCγ1 and PKCα, both downstream targets of Ca^{2+} signaling (Fig. 4*G*). Because Wnt5a was only expressed in xM cells, we looked for alternative activators of these two downstream effectors. In fact, Ca^{2+} signaling can also be activated by PDGFR in mesenchymal cells (42). Unlike Wnt5a, which was only expressed in xM cells, we demonstrated that PDGFR was expressed in both E/M and xM cells (Fig. 4*G*). This suggested the possibility, which we did not further pursue, that Ca^{2+} signaling was active independent of Wnt5a signaling in E/M cells, possibly through PDGFR signaling.

We proceeded to analyze the Wnt/PCP arm of noncanonical Wnt signaling. Wnt5a has been reported to activate Rac1, which

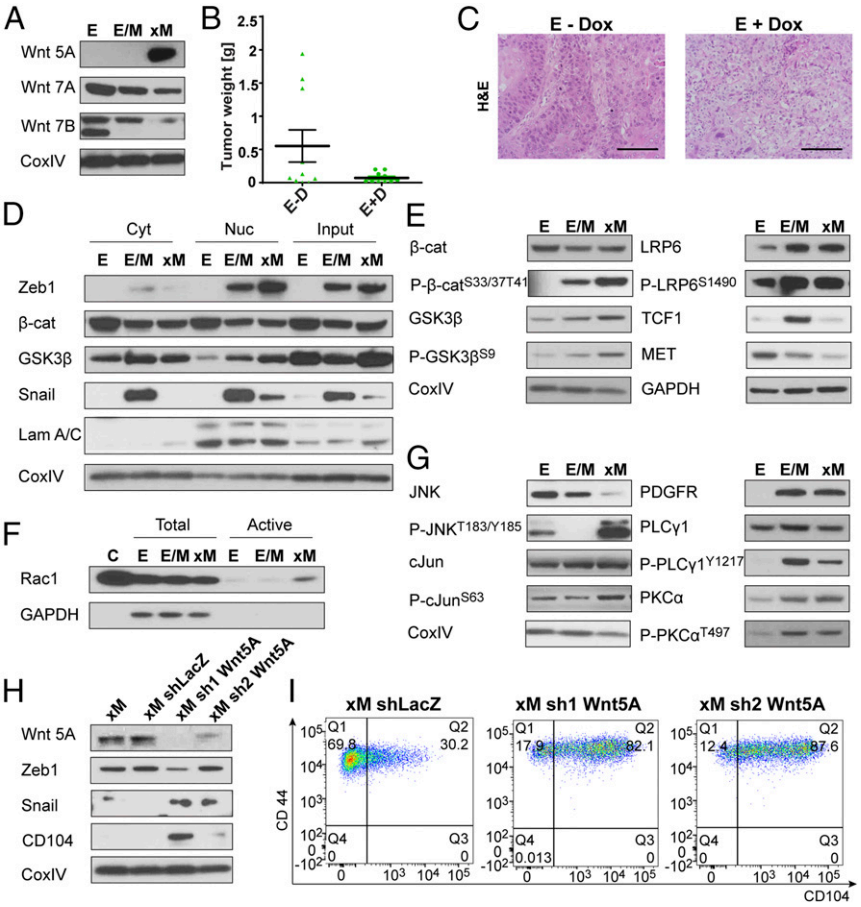

Fig. 4. Canonical Wnt signaling is active in the E/M state, whereas the xM state is maintained through Wnt5a-driven noncanonical Wnt/PCP signaling. (*A*) Western blot analysis of E, E/M, and xM cells for canonical Wnt7A/B and noncanonical Wnt5A ligand expression. (*B*) Assessment of tumor growth by tumor weight after treatment without and with Dox (D) used to induce expression of Fzd8-CRD induction in implanted epithelial (E) cells for 4 wk. Data are presented as mean ± SEM. (*C*) Analysis of tumor sections using H&E of E tumors ± Dox treatment for Fzd8-CRD induction. (*D*) Western blot analysis of cell fractionations for E, E/M, and xM cells for canonical Wnt pathway regulators and activated downstream targets. Lamin A/C staining is used as nuclear and CoxIV as cytoplasmic loading control. (*E*) Western blot analysis of E, E/M, and xM cells for canonical Wnt pathway-activated downstream targets, using CoxIV and GAPDH as loading control. (*F*) Western blot analysis PAK-PBD agarose bead pull-down assay to visualize activated Rac1 for E, E/M, and xM cells. Lysate of the positive control sample (C) was pretreated with GTPγS. (*G*) Western blot analysis of E, E/M, and xM cells for noncanonical Wnt pathway-activated downstream targets. (*H*) Western blot analysis of Wnt5A KD in xM cells. (*I*) FACS profiles for CD104 and CD44 of xM shLacZ, xM sh1Wnt5A, and xM sh2Wnt5A cell populations. (Scale bars, H&E, 10 μm.)

triggers activation of JNK and, further downstream, phosphorylation and activation of c-Jun (15). When analyzing E, E/M, and xM cells, we found that only xM cells were actively signaling through Wnt/PCP because we observed elevated levels of active-Rac1 (determined by PAK-PBD pulldown), as well as activated p-JNK and p-c-Jun by Western blot analysis with phospho-specific antibodies (Fig. 4 *F* and *G*). To summarize, we could assign noncanonical Wnt/PCP signaling specifically to the fully xM mesenchymal phenotype, clearly distinguishing it from an E/M cell state.

We also investigated whether forced Wnt5a expression could act on its own to induce cells that were previously in the E/M state to transit into the xM state. To this end, we overexpressed Wnt5a ligand in a heterogeneous $CD44^{+}$ M cell population containing subpopulations of E/M and xM cells to determine whether forced Wnt5A expression would drive a significant proportion of cells into xM phenotypic state. We did not observe a shift to an xM state by FACS analysis of CD104/CD44 marker expression, arguing that Wnt5a expression on its own is not sufficient for a phenotypic shift from the E/M to the xM state (*SI Appendix*, Fig. S6*A*).

It was also of interest to determine whether ongoing Wnt5a expression was required to maintain residence of cells in the xM state. Therefore, we infected xM cells with several shWnt5A constructs and a control shLacZ. We saw a reduction of Wnt5a protein in all cells compared with control, with shWnt5A-1 being most effective with a knockdown of almost 100% efficiency (Fig. 4*H*). Furthermore, we detected a reexpression of Snail in both knockdown lines. Consistent with these data, we observed a shift from an xM phenotype to an E/M cell state in cells expressing the Wnt5a shRNA constructs (Fig. 4*I*). These data clearly indicated that autocrine noncanonical Wnt5A signaling contributed to and was necessary for the maintenance of residence in the xM cell state.

To summarize, we could demonstrate that the highly tumorigenic E/M state is driven by and dependent on canonical Wnt signaling. However, upon transition to the xM state, canonical Wnt signaling is down-regulated, and noncanonical Wnt signaling driven by Wnt5a/PCP signaling is activated and is necessary to maintain residence in this xM state.

Discussion

Using both expression vectors and gene knockouts, we have been able to generate a population of cells that resides stably in the hybrid E/M state as defined by their expression of the CD104 and CD44 markers. These cells were created by knockout of Zeb1 and forced overexpression of Snail. The resulting cell population was

highly tumorigenic and lacked plasticity, being locked in the E/M state and unable to transit spontaneously into more E or more M states. This experimental model was able to provide direct evidence that residence in a hybrid E/M state was sufficient for maintenance of stem cell properties and that the associated stemness is exhibited independent of phenotypic plasticity.

The above experiments left several questions unanswered about the hybrid E/M cells created in this way. It is possible that this E/M cell population is itself internally heterogeneous and that use of other markers in addition to the CD104 and CD44 antigens may further stratify this E/M population and thereby resolve with far higher precision a more highly enriched or even pure subpopulation of CSCs. This notion is supported by recent data, which demonstrate that tumor cells proceed through various hybrid E/M states with differing invasive, metastatic, and differentiation characteristics (43).

xM or xE cell populations, generated either spontaneously or through experimental manipulation, show poor tumor-initiating ability. Consistent with these findings, we found that Zeb1 knockout suppressed tumorigenicity by preventing xE tumor cells from entering into an E/M state (28). Only through additional stimuli, achieved through overexpression of Snail, Twist, or Slug EMT-TFs or TGFβ-1 treatment, were Zeb1 KO cells able to advance to an E/M state. They were, however, not able to undergo a full EMT toward an xM state. Others also demonstrated in lung cancer cells, that Zeb1 KO was associated with reduced tumorigenicity and outgrowth of precursor lesions, invasion, and metastasis (31). A number of studies have further indicated that intravasation from the primary tumor and survival in the blood circulation require mesenchymal properties, whereas epithelial traits seem to be essential for the metastatic colonization of distant sites. Such reports have implied that a complete M phenotype without any option for transiting out of this state is incompatible with effective tumorigenesis and metastasis and that transient induction of an EMT program with subsequent ability of cells to transit freely between multiple E–M state leads to more aggressive phenotypes (5–7, 18, 24).

Our own results indicate that both E and M cell traits need to be coexpressed within individual carcinoma cells in order for efficient tumorigenicity to be acquired. Conversely, using comix experiments of nonplastic xE with nonplastic xM HMLER breast cancer cells, we demonstrated that these mixtures could not substitute for residence by carcinoma cells in the hybrid E/M phenotype. This indicated that the coexpression of E and M traits within individual cells, rather than the exchange of signals between E and M cells, is required for the tumor-initiating ability of carcinoma cells.

We show that high-level expression of Zeb1 (Fig. 3*B* and *SI Appendix*, Fig. S5*A*) causes cells to complete an entire EMT program, driving them into the xM state that is incompatible with efficient tumor-initiating abilities. In contrast, knockout of the *ZEB1* gene together with forced expression of either Snail, Slug, or Twist or exposure to TGF-β1 causes cells to advance from a xE state to the hybrid E/M state; such cells are unable to continue progression into the xM state. The resulting entrance into and stable residence within the E/M state yielded cells that were ∼38-fold more tumorigenic than E-SCC control cells (Fig. 3*D*). Such cells retained competence to complete their EMT programs, since full EMT and entrance into the highly mesenchymal xM state could indeed be achieved by experimental reintroduction of Zeb1 and resulting restoration of Zeb1 function.

The present work also highlights the contrasting functions of the canonical and noncanonical Wnt signaling pathways. The canonical β-catenin–dependent Wnt signaling pathway has been associated with normal and neoplastic stem cell signaling (11). In our study, we observed active canonical Wnt signaling in the hybrid E/M cell state and an up-regulated expression of the canonical Wnt7a and Wnt7b ligands, which has been shown to drive autocrine Wnt/β-catenin signaling in pancreatic cancer (44). Moreover, we found that high Snail expression observed in the E/M cells and active canonical Wnt signaling go hand in hand. Indeed, the two have been proposed to form a positive feedback loop, whereby Snail has been reported to promote canonical Wnt target gene expression and to interact physically with β-catenin (45, 46). We find that the stem programs involving high Snail and canonical Wnt signaling coexist in the tumorigenic hybrid E/M state, providing further support for the notion that the E/M state harbors the majority if not virtually all of the breast cancer stem cell pool (34, 37).

Cells that transition through a complete EMT program into the xM state switch from canonical to noncanonical, Wnt/β-catenin–independent signaling, the latter involving Wnt5a/PCP signaling. Furthermore, our studies show that ongoing expression of the noncanonical ligand, Wnt5A, is necessary to maintain residence in the poorly tumorigenic xM state and that knockdown of Wnt5A expression enables such xM cells to revert to a hybrid E/M state in which other work has demonstrated that canonical Wnt signaling is active. We note here that the ability of noncanonical Wnt5a to inhibit canonical Wnt signaling has been established in various studies of disease and development, helping to explain the distinct, mutually exclusive E/M and xM states (14, 47).

The HMLER cells used in our studies form tumors that are similar to those forming triple-negative human breast cancers (TNBCs) (19). TNBC has been associated with dysregulated expression of both canonical and noncanonical Wnt signaling pathways (48) and displays tumor cells of various phenotypic stages of the EMT program (49). The present findings suggest that the design of future therapeutic approaches will need to consider the various distinct E and M subpopulations of carcinoma cells in these tumors, as well as the plasticity of such cells residing in different positions along the E–M spectrum. Efforts at targeting mesenchymal HMLER cells by reverting them back to a more differentiated epithelial phenotype have shown significant effects on tumor growth (50, 51). Several small molecules blocking Wnt signaling as well as decoy receptors antagonizing Wnt signaling, the latter employing Fc-fused-Fz8CRD (17), are currently in clinical trials. Indeed, as shown here, Fz8CRD expression also efficiently reduced tumor growth in the HMLER cell model. Therefore, we propose that a combination therapy of drugs promoting mesenchymal–epithelial transition (MET) together with Wnt signaling inhibitors targeting the aggressive/stem-like E/M state may prove effective in treating highly heterogeneous cancers such as TNBCs.

Materials and Methods

Cell Lines and Culture Conditions. HMLER and SUM149 cells were cultured as described (19). The generation of the different cell lines is outlined in detail in *SI Appendix, SI Materials and Methods*, including the plasmid and virus construction.

FACS Analyses and Sorting. HMLER cells were trypsinized and tumors dissociated using a tumor isolation kit (Milteny). One million single cells in suspensions per 100 μL were stained with appropriate antibody dilution (*SI Appendix, SI Materials and Methods*) in 2% IFS/PBS for 15–30 min RT in the dark. DAPI was used for live–dead analysis. Cells were directly resuspended in PBS and analyzed on a LSRII flow and sorted on a FACS Aria (BD Biosciences). Data were analyzed using the FlowJo software (Tree Star). To purify the $CD104^+$ and $CD104^-$ populations the top 5% of the positive and negative spectrum were isolated.

RNA-Seq. Q-PCR was performed as described before (19) (*SI Appendix, Supplementary Materials and Methods*). RNA-Seq libraries were prepared using the TruSeq-stranded polA mRNA kits (Illumina). Libraries were pooled and sequenced on the HiSeq 2500 sequencer, 40 bp reads to a depth of ∼40–45 million mapped. RNA-Seq data from this study have been deposited at GEO under accession number GSE119149. RNA-Seq paired-end reads from Illumina 1.5 encoding were aligned using TopHat (v.2.0.12) (52) to the human genome (GRCh37) with Ensemble annotation (GRCh37.75) in gtf format. Differentially expressed genes were hierarchical clustered using uncentered

correlation in Cluster3 (53) on z-scores obtained from normalized counts. Clusters were analyzed for significant overrepresentation of GO terms. Significantly changing EMT-TFs and Wnt ligands and receptors were grouped manually.

Active-Rac1-Pulldown, Nuclear Fractionation, and Western Blotting. Active-Rac1-pulldown with PAK-PBD agarose beads was performed using the Rac1 Activation Assay following manufacturer's instructions (Cell Biolabs). Nuclear fractionation and Western blotting details are described in *SI Appendix, SI Materials and Methods*.

IF and Histology Analysis. IF analyses on cells and tissues were performed as described before (54, 55) and outlined in *SI Appendix, SI Materials and Methods*. For Zeb1 staining on tissues an amplification step using the TSA Plus Kit (PerkinElmer) was performed according to manufactures instructions. Slides were mounted in ProLong Gold antifade reagent (Invitrogen).

Animal Studies. All studies involving animals have been approved and complied with the guidelines of the Massachusetts Institute of Technology (MIT) Committee on Animal Care. For orthotopic xenograft transplants, 100,000 cells in 20% matrigel/MEGM were injected into NOD/SCID mice into the mammary fat pad. For limiting dilution assays, 1 million, 100,000, and 10,000 cells in 20% matrigel/MEGM were injected s.c. into NOD/SCID mice. Tumors were extracted after 8 wk and analyzed by weight, size, and single-cell FACS analysis. The in vivo Dox treatment was administered through drinking water containing 2 mg/mL Dox and 10 mg/mL sucrose.

ACKNOWLEDGMENTS. We thank Christine Chaffer, Whitney Henry, Diwakar Pattabiraman, and Arthur Lambert for critical comments and suggestions, as well as Zuzanna Keckesova, Jasmine Whyte, Tsukasa Shibue, and Yun Zhang for critical discussion on the manuscript. We further thank the Flow Cytometry Core Facility, the Genome Technology Core, and the Bioinformatics and Research Computing Core at the Whitehead Institute for Biomedical Research and at the MIT Koch Institute. This work was supported by the Leopoldina Forschungsgemeinschaft and the National Institutes of Health (Grants R01 CA078461 and U01 CA184897). R.A.W. is an American Cancer Society Research Professor and a Daniel K. Ludwig Foundation Cancer Research Professor.

1. Brooks MD, Burness ML, Wicha MS (2015) Therapeutic implications of cellular heterogeneity and plasticity in breast cancer. *Cell Stem Cell* 17:260–271.
2. Nieto MA, Huang RY, Jackson RA, Thiery JP (2016) Emt: 2016. *Cell* 166:21–45.
3. Thiery JP (2002) Epithelial-mesenchymal transitions in tumour progression. *Nat Rev Cancer* 2:442–454.
4. Brabletz T (2012) To differentiate or not—Routes towards metastasis. *Nat Rev Cancer* 12:425–436.
5. Schmidt JM, et al. (2015) Stem-cell-like properties and epithelial plasticity arise as stable traits after transient Twist1 activation. *Cell Rep* 10:131–139.
6. Tran HD, et al. (2014) Transient SNAIL1 expression is necessary for metastatic competence in breast cancer. *Cancer Res* 74:6330–6340.
7. Tsai JH, Donaher JL, Murphy DA, Chau S, Yang J (2012) Spatiotemporal regulation of epithelial-mesenchymal transition is essential for squamous cell carcinoma metastasis. *Cancer Cell* 22:725–736.
8. Lamouille S, Xu J, Derynck R (2014) Molecular mechanisms of epithelial-mesenchymal transition. *Nat Rev Mol Cell Biol* 15:178–196.
9. Alexander CM, Goel S, Fakhraldeen SA, Kim S (2012) Wnt signaling in mammary glands: Plastic cell fates and combinatorial signaling. *Cold Spring Harb Perspect Biol* 4: a008037.
10. Zeng YA, Nusse R (2010) Wnt proteins are self-renewal factors for mammary stem cells and promote their long-term expansion in culture. *Cell Stem Cell* 6:568–577.
11. Reya T, Clevers H (2005) Wnt signalling in stem cells and cancer. *Nature* 434:843–850.
12. Gujral TS, et al. (2014) A noncanonical Frizzled2 pathway regulates epithelial-mesenchymal transition and metastasis. *Cell* 159:844–856.
13. Weeraratna AT, et al. (2002) Wnt5a signaling directly affects cell motility and invasion of metastatic melanoma. *Cancer Cell* 1:279–288.
14. Asem MS, Buechler S, Wates RB, Miller DL, Stack MS (2016) Wnt5a signaling in cancer. *Cancers (Basel)* 8:E79.
15. Niehrs C (2012) The complex world of WNT receptor signalling. *Nat Rev Mol Cell Biol* 13:767–779.
16. Nusse R, Clevers H (2017) Wnt/β-catenin signaling, disease, and emerging therapeutic modalities. *Cell* 169:985–999.
17. Zhan T, Rindtorff N, Boutros M (2017) Wnt signaling in cancer. *Oncogene* 36: 1461–1473.
18. Celià-Terrassa T, et al. (2012) Epithelial-mesenchymal transition can suppress major attributes of human epithelial tumor-initiating cells. *J Clin Invest* 122:1849–1868.
19. Bierie B, et al. (2017) Integrin-β4 identifies cancer stem cell-enriched populations of partially mesenchymal carcinoma cells. *Proc Natl Acad Sci USA* 114:E2337–E2346.
20. Hong T, et al. (2015) An Ovol2-Zeb1 mutual inhibitory circuit governs bidirectional and multi-step transition between epithelial and mesenchymal states. *PLOS Comput Biol* 11:e1004569.
21. Jolly MK, et al. (2015) Implications of the hybrid epithelial/mesenchymal phenotype in metastasis. *Front Oncol* 5:155.
22. Jolly MK, et al. (2016) Stability of the hybrid epithelial/mesenchymal phenotype. *Oncotarget* 7:27067–27084.
23. Tam WL, Weinberg RA (2013) The epigenetics of epithelial-mesenchymal plasticity in cancer. *Nat Med* 19:1438–1449.
24. Lambert AW, Pattabiraman DR, Weinberg RA (2017) Emerging biological principles of metastasis. *Cell* 168:670–691.
25. Elenbaas B, et al. (2001) Human breast cancer cells generated by oncogenic transformation of primary mammary epithelial cells. *Genes Dev* 15:50–65.
26. Hahn WC, et al. (2002) Enumeration of the simian virus 40 early region elements necessary for human cell transformation. *Mol Cell Biol* 22:2111–2123.
27. Serrano-Gomez SJ, Maziveyi M, Alahari SK (2016) Regulation of epithelial-mesenchymal transition through epigenetic and post-translational modifications. *Mol Cancer* 15:18.
28. Chaffer CL, et al. (2013) Poised chromatin at the ZEB1 promoter enables breast cancer cell plasticity and enhances tumorigenicity. *Cell* 154:61–74.
29. Orimo A, et al. (2005) Stromal fibroblasts present in invasive human breast carcinomas promote tumor growth and angiogenesis through elevated SDF-1/CXCL12 secretion. *Cell* 121:335–348.
30. Kojima Y, et al. (2010) Autocrine TGF-beta and stromal cell-derived factor-1 (SDF-1) signaling drives the evolution of tumor-promoting mammary stromal myofibroblasts. *Proc Natl Acad Sci USA* 107:20009–20014.
31. Krebs AM, et al. (2017) The EMT-activator Zeb1 is a key factor for cell plasticity and promotes metastasis in pancreatic cancer. *Nat Cell Biol* 19:518–529.
32. Thiery JP, Acloque H, Huang RYJ, Nieto MA (2009) Epithelial-mesenchymal transitions in development and disease. *Cell* 139:871–890.
33. Guaita S, et al. (2002) Snail induction of epithelial to mesenchymal transition in tumor cells is accompanied by MUC1 repression and ZEB1 expression. *J Biol Chem* 277: 39209–39216.
34. Ye X, et al. (2015) Distinct EMT programs control normal mammary stem cells and tumour-initiating cells. *Nature* 525:256–260.
35. Yu H, Ye X, Guo N, Nathans J (2012) Frizzled 2 and frizzled 7 function redundantly in convergent extension and closure of the ventricular septum and palate: Evidence for a network of interacting genes. *Development* 139:4383–4394.
36. Smallwood PM, Williams J, Xu Q, Leahy DJ, Nathans J (2007) Mutational analysis of Norrin-Frizzled4 recognition. *J Biol Chem* 282:4057–4068.
37. Clevers H, Loh KM, Nusse R (2014) Stem cell signaling. An integral program for tissue renewal and regeneration: Wnt signaling and stem cell control. *Science* 346:1248012.
38. Caspi M, Zilberberg A, Eldar-Finkelman H, Rosin-Arbesfeld R (2008) Nuclear GSK-3beta inhibits the canonical Wnt signalling pathway in a beta-catenin phosphorylation-independent manner. *Oncogene* 27:3546–3555.
39. Stamos JL, Weis WI (2013) The β-catenin destruction complex. *Cold Spring Harb Perspect Biol* 5:a007898.
40. Roose J, et al. (1999) Synergy between tumor suppressor APC and the beta-catenin-Tcf4 target Tcf1. *Science* 285:1923–1926.
41. Scheel C, et al. (2011) Paracrine and autocrine signals induce and maintain mesenchymal and stem cell states in the breast. *Cell* 145:926–940.
42. Tam WL, et al. (2013) Protein kinase C α is a central signaling node and therapeutic target for breast cancer stem cells. *Cancer Cell* 24:347–364.
43. Pastushenko I, et al. (2018) Identification of the tumour transition states occurring during EMT. *Nature* 556:463–468.
44. Arensman MD, et al. (2014) WNT7B mediates autocrine Wnt/β-catenin signaling and anchorage-independent growth in pancreatic adenocarcinoma. *Oncogene* 33: 899–908.
45. Stemmer V, de Craene B, Berx G, Behrens J (2008) Snail promotes Wnt target gene expression and interacts with beta-catenin. *Oncogene* 27:5075–5080.
46. Yook JI, et al. (2006) A Wnt-Axin2-GSK3beta cascade regulates Snail1 activity in breast cancer cells. *Nat Cell Biol* 8:1398–1406.
47. Veeman MT, Axelrod JD, Moon RT (2003) A second canon. Functions and mechanisms of beta-catenin-independent Wnt signaling. *Dev Cell* 5:367–377.
48. Pohl SG, et al. (2017) Wnt signaling in triple-negative breast cancer. *Oncogenesis* 6: e310.
49. Marusyk A, Almendro V, Polyak K (2012) Intra-tumour heterogeneity: A looking glass for cancer? *Nat Rev Cancer* 12:323–334.
50. Keckesova Z, et al. (2017) LACTB is a tumour suppressor that modulates lipid metabolism and cell state. *Nature* 543:681–686.
51. Pattabiraman DR, et al. (2016) Activation of PKA leads to mesenchymal-to-epithelial transition and loss of tumor-initiating ability. *Science* 351:aad3680.
52. Kim D, et al. (2013) TopHat2: Accurate alignment of transcriptomes in the presence of insertions, deletions and gene fusions. *Genome Biol* 14:R36.
53. de Hoon MJ, Imoto S, Nolan J, Miyano S (2004) Open source clustering software. *Bioinformatics* 20:1453–1454.
54. Kröger C, et al. (2013) Keratins control intercellular adhesion involving PKC-α-mediated desmoplakin phosphorylation. *J Cell Biol* 201:681–692.
55. Kröger C, et al. (2011) Placental vasculogenesis is regulated by keratin-mediated hyperoxia in murine decidual tissues. *Am J Pathol* 178:1578–1590.

Correction

CELL BIOLOGY

Correction for "Acquisition of a hybrid E/M state is essential for tumorigenicity of basal breast cancer cells," by Cornelia Kröger, Alexander Afeyan, Jasmin Mraz, Elinor Ng Eaton, Ferenc Reinhardt, Yevgenia L. Khodor, Prathapan Thiru, Brian Bierie, Xin Ye, Christopher B. Burge, and Robert A. Weinberg, which was first published March 25, 2019; 10.1073/pnas.1812876116 (*Proc. Natl. Acad. Sci. U.S.A.* **116**, 7353–7362).

The authors wish to note the following: "During the assembly of this manuscript, the authors inadvertently placed duplicated images of the hematoxylin and eosin (H&E) staining of the E-SCC-Zeb1KO tumors of Fig. 2*D* into Fig. 3*E* E-SCC-Zeb1KO and E-SCC-ZEB1KOSn. The duplicate images have now been replaced with the originally intended images. This correction does not affect any result described in the figures and does not alter the message of the manuscript in any way. We apologize for any inconvenience that this error may have caused readers." The corrected Fig. 3 and its legend appear below.

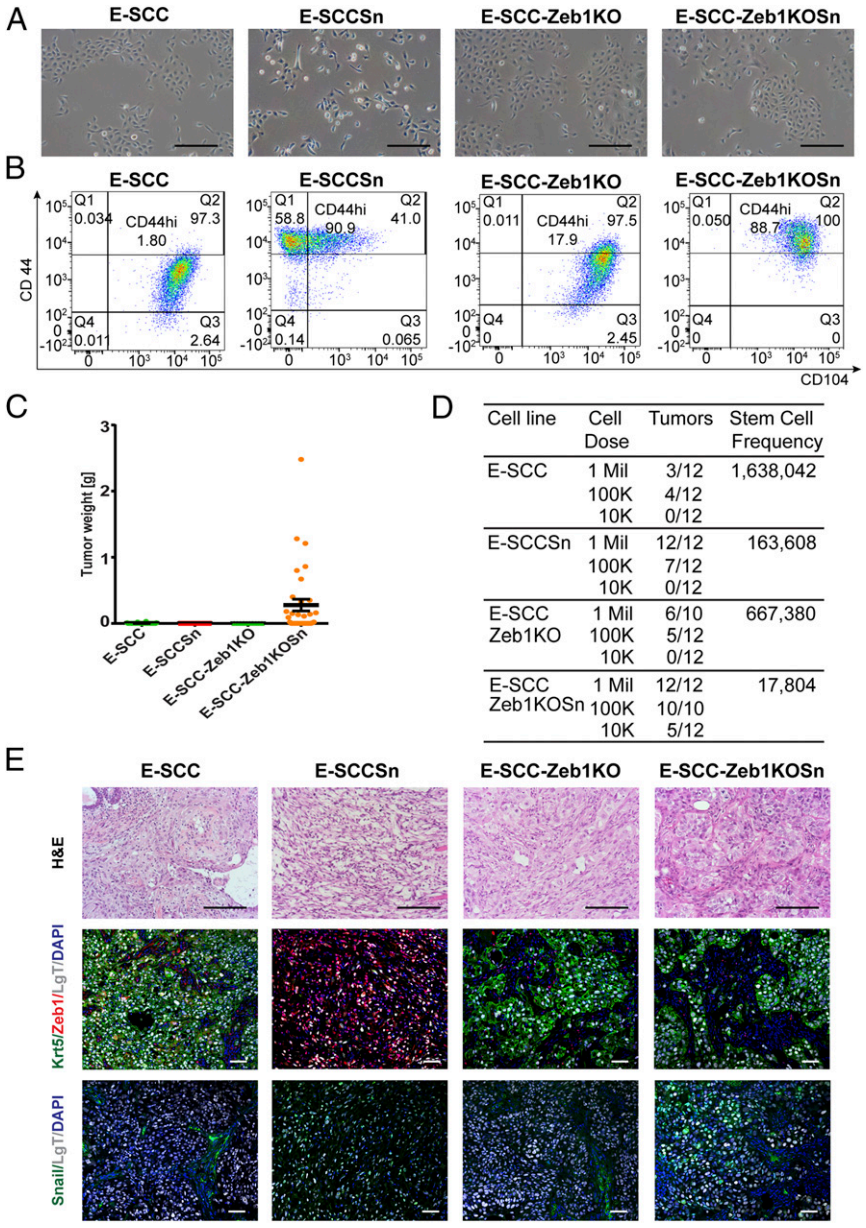

Fig. 3. Zeb1 is needed for a complete EMT, but the hybrid E/M cell state is sufficient for tumor formation. (*A*) Representative images of cell morphology of E-SCC, E-SCCSn, E-SCC-Zeb1KO, and E-SCC-Zeb1KOSn cells by phase contrast (brightfield) microscopy. (*B*) FACS profiles for CD104 and CD44 of E-SCC, E-SCCSn, E-SCC-Zeb1KO, and E-SCC-Zeb1KOSn populations. (*C*) Assessment of tumorigenicity and tumor growth by tumor weight of orthotopic injection E-SCC, E-SCCSn, E-SCC-Zeb1KO, and E-SCC-Zeb1KOSn populations. Data are presented as mean ± SEM (*D*) Differences in tumor-initiating ability of E-SCC, E-SCCSn, E-SCC-Zeb1KO, and E-SCC-Zeb1KOSn cells upon transplantation at limiting dilutions into NOD/SCID mice. (*E*) Analysis of E-SCC, E-SCCSn, E-SCC-Zeb1KO, and E-SCC-Zeb1KOSn tumor sections using H&E and IF staining for Krt/Zeb1 or Snail. LgT staining was used to differentiate tumor cells from mouse stromal cells. Nucleus is visualized by DAPI staining. (Scale bars, brightfield; H&E, 10 μm; IF, 2 μm in *E*.)

Published online May 28, 2019.

www.pnas.org/cgi/doi/10.1073/pnas.1907473116